Int. J. Electrochem. Sci., 7 **(2012)** 11206 - 11218

International Journal of
ELECTROCHEMICAL
SCIENCE
www.electrochemsci.org

A Novel Tri-Protein Bio-Interphase Composed of Cytochrome *c*, Horseradish Peroxidase and Concanavalin A: Electron Transfer and Electrocatalytics

Yonghai Song[1,2], *Yu Wang*[2], *Hongyu Liu*[2] *and Li Wang*[1,2,*]

[1] Key Laboratory of Functional Small organic molecule, Ministry of Education, Jiangxi Normal University, Nanchang 330022, People's Republic of China
[2] College of Chemistry and Chemical Engineering, Jiangxi Normal University, Nanchang 330022, People's Republic of China
[*]E-mail: lwangsy2003@hotmail.com

Received: 24 September 2012 / *Accepted:* 19 October 2012 / *Published:* 1 November 2012

A tri-protein bio-interphase composed of concanavalin A (Con A), cytochrome *c* (Cyt *c*) and horseradish peroxidase (HRP) was developed by layer-by-layer assembly of HRP, Con A, mixture of Cyt *c* and HRP. The assembly uses lectin-sugar biospecific interactions between Con A and HRP on biocompatible 11-mercaptoundecanoic acid-6-mercapto-1-hexanol modified gold electrode. This novel tri-protein bio-interphase is used as a model system to mimic the electron transfer and electrocatalytic performance of the proteins in living organisms. The tri-protein bio-interphase was characterized by the atomic force microscopy, electrochemical impedance spectroscopy, cyclic voltammetry and amperometry. The fast electron transfer rate at the bio-interphase indicated synergistic interactions between the involved proteins. Moreover, due to the good electrocatalytic response the tri-protein bio-interphase can be used as hydrogen peroxide (H_2O_2) and oxygen (O_2) sensor. This study also provides new insights for the electron transfer of multi-proteins in a bio-interphase and the development of biosensors.

Keywords: Electron transfer; Concanavalin A; Horseradish peroxidase; Cytochrome *c*; H_2O_2

1. INTRODUCTION

A bio-interphase composed of proteins is particularly interesting not only for analytical application but also for better understanding synergistic mechanism of enzymatic reactions in the living systems [1-10]. A series of bi-protein bio-interphases containing cytochrome *c* (Cyt *c*) and enzymes (such as blue copper, sulfite oxidase, HRP, etc.) have been developed by incorporating these two proteins into polyelectrolyte multilayer to mimic the sequential electron transfer in real biological

systems or to fabricate novel biosensors and biodevices [11-20]. As a well characterized electron-transfer protein, Cyt *c* has been used extensively as a test system for direct electron transfer (DET) of redox proteins and communication in a protein matrix [21-23]. It was found that a multi-step electron transfer chain can be formed from the electrode via the Cyt *c* layers towards enzymes and finally to analyses [14]. To avoid the disruption of abiological materials in these bio-interphases to the electron transfer, multiprotein co-assembly technique was developed, for example, mediator-free electron transfer of the enzymes within the bio-interphase was achieved, through layer-by-layer assembly of the redox protein Cyt *c* with sulfite oxidase, by taking advantage of direct interactions between the two functional biocomponents [15]. Although electrostatic interactions between these two proteins were found to be sufficient for layer-by-layer deposition of components, the reproducibility and stability of multiprotein bio-interphase remained unsatisfactory. Our recent work indicated that DNA network as a matrix for the alternate assembling of HRP and Cyt *c* could improve the reproducibility and stability of the bio-interphase [24]. However, the DNA molecules are similar with polyelectrolyte and did not play a role in the interaction between proteins in real biological systems due to its existence inside cell nucleus.

Concanavalin A (Con A) is one of the lectin proteins found in Jack bean and exists as a tetramer with a molecular mass of 104000 [25]. It could be used as a versatile platform to immobilize a variety of glyenzymes on a solid support. HRP can be assembled into multilayer without any chemical modification by the alternate deposition of Con A and the native enzymes, through specific binding of Con A and sugar residues of the enzymes [26-28], which inspired us to construct a novel multi-protein bio-interphase by using Con A as a scaffold.

In this study, a novel tri-protein bio-interphase was developed through layer-by-layer assembling HRP, Con A and Cyt *c*-HRP on gold (Au) electrode which was pre-modified with biocompatible 11-mercaptoundecanoic acid (MUA)- 6-mercapto-1-hexanol (MCH) mixed SAMs. HRP was firstly assembled on MUA-MCH/Au electrode based on electrostatic interactions to provide sugar residues. Then Con A molecules were assembled on the HRP/MUA-MCH/Au electrode based on sugar-lectin biospecific interactions with HRP [29,30]. Finally, the Cyt *c*-HRP mixture was co-immobilized on the Con A/HRP/MUA-MCH/Au electrode through specific binding of Con A and HRP and electrostatic interactions between HRP and Cyt *c*. The novel tri-protein bio-interphase was formed as a model system to study the mechanism of multienzyme-catalyzed reactions.

2. EXPERIMENTAL

2.1 Reagents and materials

Cytochrome *c* (Cyt *c*, 98%), horseradish peroxidase (HRP), concanavalin A (Con A) from canavalia ensiformis, 11-mercaptoundecanoic acid (MUA, 95%) and 6-mercapto-1-hexanol (MCH, 97%) were purchased from Sigma-Aldrich and used as received. Other analytical grade reagents were purchased from Beijing Chemical Reagent Factory (Beijing, China). The supporting electrolyte (pH 9.6) was prepared by mixing 0.05 M $Na_2B_4O_7$ and 0.2 M NaOH. The pH 7.0 (0.2 M) phosphate buffer

solution (PBS) was prepared by mixing Na_2HPO_4 (0.2 M) and NaH_2PO_4 (0.2 M). All solutions were prepared with ultra-pure water purified by a Millipore-Q System (18.2 MΩ.cm). 80 μM HRP solution was made in PBS (pH 7.0). 80 μM Con A solution was made in PBS (pH 7.0) containing 1 mM $CaCl_2$ and $MnCl_2$. 400 μM Cyt *c* and 110 μM HRP mixed solution was made in supporting electrolyte of $Na_2B_4O_7$ and NaOH.

2.2 Preparation of the modified electrode

The pretreated Au electrode was firstly immersed in a mixed ethanol solution of MUA (100 μM) and MCH (1.0 mM) for 12 h to form a self-assembled monolayers (SAMs) on the bare electrode. Then, 5 μL HRP (80 μM), Con A (80 μM) and mixture of Cyt *c* (400 μM) and HRP (110 μM) were sequentially casted onto the MUA-MCH/Au surface, each with immediate drying at 4 ºC for 4 h and rinsed with ultra-pure water. The drying step is necessary in the LBL assembly, to get stable films, while rinsing is also necessary to remove weakly bound molecules. Finally the electrode was stored at 4 ºC for further use. The detailed modification process of the electrode is shown in Fig. 1.

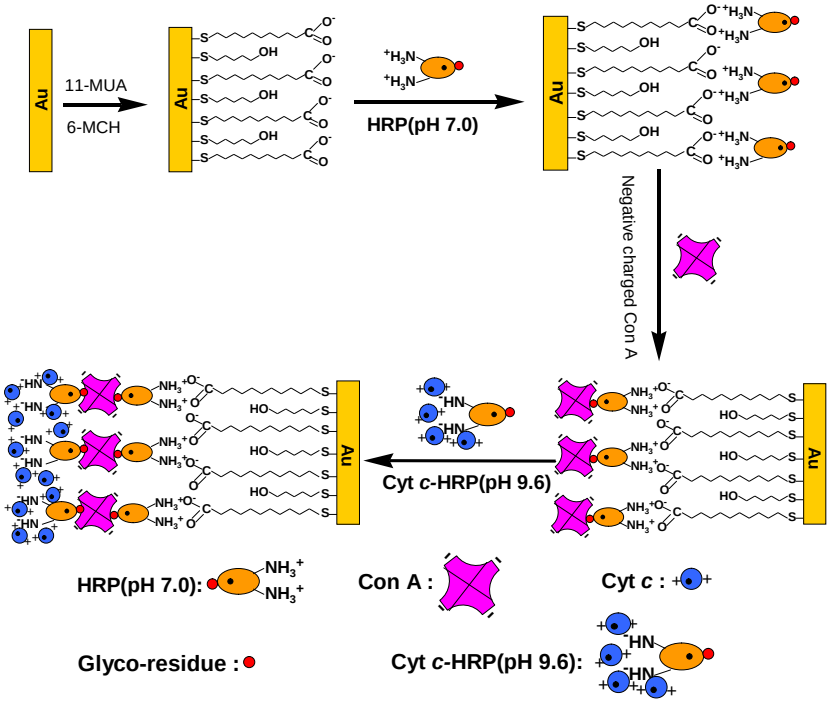

Figure 1. Schematic representation of the electrode construction process.

2.3 Apparatus

All electrochemical experiments were performed with a CHI 750D electrochemical workstation (Shanghai Chenhua Instruments Co., China). A three-electrode configuration was used with the modified Au electrode as the working electrode, a platinum wire as the auxiliary electrode, and a saturated calomel electrode (SCE) as the reference electrode. Cyclic voltammetric experiments were

carried out in 10.0 mL supporting electrolyte solution (pH 9.6), which were purged with high purity nitrogen prior to experiments and blanketed with nitrogen during electrochemical experiments.

Atomic force microscopy (AFM) measurements were carried out with an AJ-III Instrument (Shanghai Aijian Nanotechnology Co., China) under tapping mode. Standard silicon cantilevers (spring constant 0.6–6 N m^{-1}) were used at their resonance frequency (typically, 60–150 kHz). All AFM images were acquired under ambient conditions, and images were raw data except for flattening. Au thin films were formed on the oxidized silicon wafer by electron beam evaporation under 10^{-6} Torr pressure and used as substrates for AFM imaging. All experiments were performed at an ambient temperature of 20±2°C.

3. RESULTS AND DISCUSSION

3.1 AFM characterization of the tri-protein bio-interphase modified electrodes

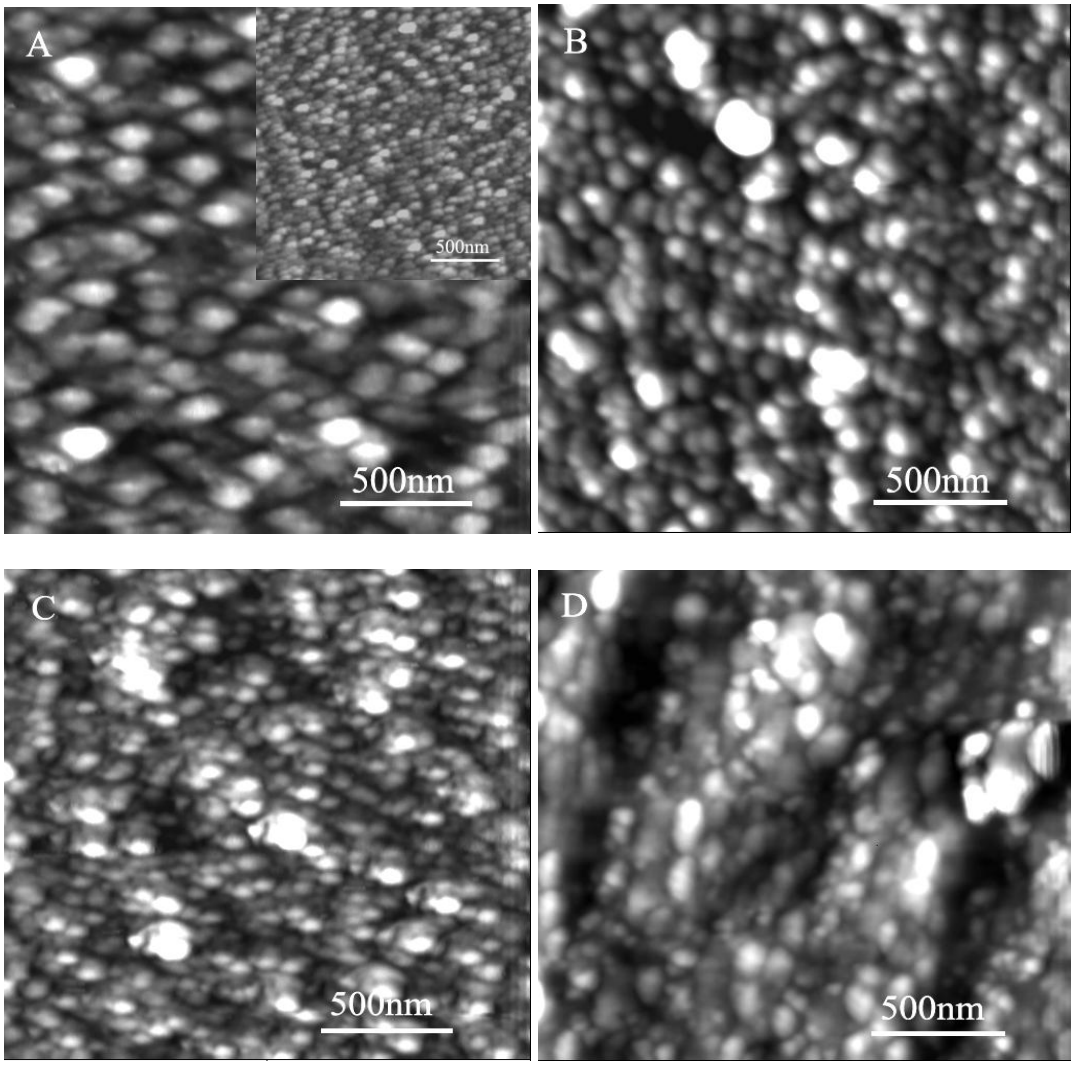

Figure 2. AFM images of MUA-MCH/Au (A), HRP/MUA-MCH/Au (B), Con A/HRP/MUA-MCH/Au (C) and Cyt *c*-HRP/Con A/HRP/MUA-MCH/Au (D). The z range are 8 nm (A-C) and 20 nm (D), respectively. Inset in Fig. 2A was AFM image of the bare Au substrate.

To study the surface morphology of the construction process of the tri-protein bio-interphase modified electrode on a micro-scale, AFM is considered to be an excellent tool. Fig. 2 show the typical AFM images of differently modified electrodes. The AFM image depicted in Fig. 2A showed some nanoparticles (NPs), characteristic of Au NPs from the bare Au substrate (Inset in Fig. 2A) [24]. After HRP assembled, small dots appeared and uniformly dispersed on the surface (Fig. 2B). The height of these dots is about 2.1 ± 0.6 nm, which was similar to the size of one HRP molecule [31]. After the HRP/MUA-MCH/Au sample was further immersed in the Con A solution for 4 h in a separate experiment, Con A molecules were assembled on the surface by the specific binding of Con A and HRP (small dots near HRP as shown in Fig. 2C). The AFM image of Cyt *c*-HRP/Con A/HRP/MUA-MCH/Au revealed the uniform distribution of Cyt *c*-HRP on the Con A/HRP/MUA-MCH/Au surface (Fig. 2D). The isoelectric point of HRP is 8.9 [31] and 9.8 for the Cyt *c* [3] therefore, at pH 9.6, HRP and Cyt *c* can make a positively charged complex through electrostatic interactions (as shown in Fig. 1). The resulted complex could efficiently assemble on Con A/HRP/MUA-MCH/Au surface due to the specific binding and electrostatic interactions between Con A and HRP to form Cyt *c*-HRP/Con A/HRP/MUA-MCH/Au electrode.

3.2 Electrochemical behaviors of the tri-protein modified electrodes

Electrochemical impendence spectroscopy (EIS) with 5 mM $[Fe(CN)_6]^{3-/4-}$ as the electroactive probe and 0.1 M KCl as the supporting electrolyte was used to monitor and confirm the modification of bare Au electrode (Fig. 3A). To give more detailed information about the electrical properties of these modified electrodes, the Randles circuit (inset, Fig. 3A) was chosen to fit the impedance data [32]. In the Randles circuit, the resistance to charge transfer (R_{ct}) and the diffusion impedance (W) were both assumed in parallel to the interfacial capacity (C_{dl}). This parallel structure of R_{ct} and C_{dl} gave rise to a semicircle in the complex plane plot of Z_{im} against Z_{re}. For bare Au electrode, the EIS response of $Fe(CN)_6^{3-/4-}$ exhibited a Warburg line in a very wide frequency range, characteristic of a diffusion-controlled electrochemical process. R_{ct} was calculated to be 0.11 KΩ cm^2 on this electrode (curve a). After the step-by-step assembly of MUA-MCH SAMs, HRP, Con A, and mixture of Cyt *c*-HRP on the Au surface, a semi circle in the high-frequency domain were observed since these multilayers behaved as a physical barrier and blocked or limited the access of the probe to the electrode surface. And R_{ct} was increased to be 4.7 KΩ cm^2 on the MUA-MCH/Au (curve b), 6.8 KΩ cm^2 on the HRP/MUA-MCH/Au (curve c), 9.3 KΩ cm^2 on the Con A/HRP/MUA-MCH/Au (curve d), 10.9 KΩ cm^2 on the Cyt *c*-HRP/Con A/HRP /MUA-MCH/Au (curve e), 11.8 KΩ cm^2 on the Cyt *c*/Con A/HRP/MUA-MCH/Au (curve f) and 13.1 KΩ cm^2 on the HRP/Con A/HRP/MUA-MCH/Au (curve g), respectively. R_{ct} becomes larger, indicating that the interfacial charge transfer of the probe becomes more difficult. These data showed that these various molecules were successfully assembled on the Au electrode surface and inhibited electron transfer. It is noticeable that R_{ct} for the Cyt *c*-HRP/Con A/HRP/MUA-MCH/Au (curve e) was smaller than that of the Cyt *c*/Con A/HRP/MUA-MCH/Au (curve f) and the HRP/Con A/HRP /MUA-MCH/Au (curve g), suggesting that the positively charged complex of Cyt *c* and HRP resulted in a porous structure to enhance the electron transfer.

Fig. 3B shows cyclic voltammograms (CVs) of different electrodes in 10.0 mL supporting electrolyte solution (pH 9.6) at a scan rate of 0.1 V s^{-1}. No current was observed at the HRP/MUA-MCH/Au (curve a), the Con A/HRP/MUA-MCH/Au (curve b) and the HRP/Con A/HRP/MUA-MCH/Au (curve c). A pair of quasi-reversible peak with a peak to peak separation ($\Delta E_p = E_{pa} - E_{pc}$) of 61 mV was observed at the Cyt *c*-HRP/MUA-MCH/Au electrode (curve d). Cyt *c*/Con A/HRP/MUA-MCH/Au electrode also showed a pair of stronger redox peak with a ΔE_p of 65 mV (curve e). After the mixed proteins of Cyt *c* and HRP were co-entrapped on the Con A/HRP/MUA-MCH/Au electrode, the ΔE_p decreased to 56 mV (curve f), smaller than our previous result [18]. The peak current was larger than that of the other electrodes. The results indicated that the co-entrapped Cyt *c*-HRP in tri-protein bio-interphase could greatly promote the electron transfer between proteins and the electrode. It was because that the sugar-lectin biospecific interaction between HRP and Con A provided a stable immobilization of Cyt *c*-HRP and the synergistic interactions between these two proteins resulted in optical conformation and a porous structure. According to previous results for the arrangement of Cyt *c* and sulfonated polyaniline [23] and LBL arrangement of Cyt *c* and sulfite oxidase [15], long-distance electron transfer process might be ascribed to one of the following mechanisms: (1) electron transfer occurred by direct interaction between neighboring Cyt *c* or HRP molecules, while Con A wass responsible for stabilization of the arrangement; (2) Cyt *c* and HRP could be wired by Con A, which would be a conductive polymer under specific conditions; (3) electron transfer occurred by a face-to-face electron hopping between Cyt c and HPR or Cyt *c*.

The effect of the ratio of Cyt *c* and HRP ($n_{Cyt\ c}/n_{HRP}$) on the electron transfer between mixed proteins and underlying electrode was also investigated by CVs. As shown in Fig. 3C, a remarkable change of peak currents was observed as the $n_{Cyt\ c}/n_{HRP}$ varied from 1:1 to 7:1. The peak current increased initially with the $n_{Cyt\ c}/n_{HRP}$ in the range of 1:1 to 4:1 and reached the maximum at 4:1. As the $n_{Cyt\ c}/n_{HRP}$ further increased, the peak current tended to be decreased gradually. The result was likely because the interaction between Cyt *c* and HPR changed the coordination in axial direction of the heme to obtain favorable conformation for electron transfer [33]. If the electron transfer occurred by a face-to-face electron hopping between Cyt *c* and HRP or Cyt *c* molecules, the $n_{Cyt\ c}/n_{HRP}$ has no effect on the electron transfer. Therefore, this experiment not only confirmed the CVs data for a synergistic interaction between Cyt *c* and HRP but also indicated the direct interaction between Cyt *c* and HRP molecules as a dominating electron transfer mechanism. Furthermore, the effect of the total mole of Cyt *c* and HRP ($n_{Cyt\ c+HRP}$) on the electron transfer between the mixed proteins and underlying electrode was also investigated. As shown in Fig. 3D, a remarkable change of peak currents was observed as the $n_{Cyt\ c+HRP}$ varied in the range of 1.3 nmol to 2.5 nmol. The peak current increased initially with the increase of the $n_{Cyt\ c+HRP}$ and reached the maximum at 2.0 nmol. Further to increase the $n_{Cyt\ c+HRP}$, the peak current tended to be decreased on the contrary. The decrease might be ascribed to the thick and dense Cyt *c*-HRP layer in the bio-interphase, especially the protein part of Cyt *c*-HRP, which hindered the electron transfer. The compacted structure of the tri-protein bio-interphase with large number of Cyt *c*-HRP might also hinder electron transfer. This experiment not only denied a face-to-face electron hopping between Cyt *c* and HPR or Cyt *c* but also confirmed the three-dimensional porous structure played a crucial role in the long-distance electron transfer.

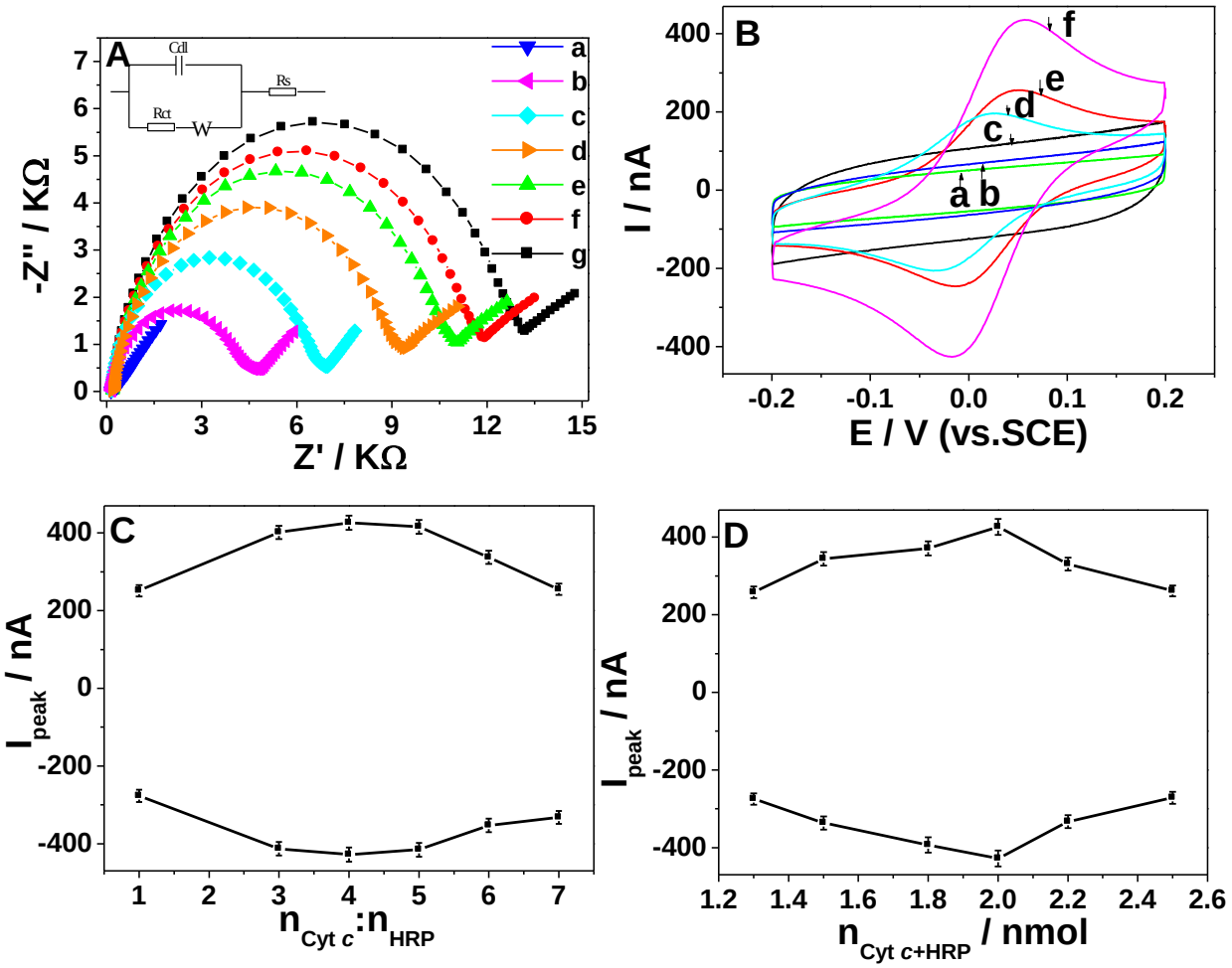

Figure 3.(A) Impendence plots of bare Au (a), MUA-MCH/Au (b), HRP/MUA-MCH/Au (c), Con A/HRP/MUA-MCH/Au (d), Cyt *c*-HRP/Con A/HRP/MUA-MCH/Au (e), Cyt *c*/Con A/HRP/MUA-MCH/Au (f) and HRP/Con A/HRP/MUA-MCH/Au (g) in the presence of 5 mM $Fe(CN)_6^{3-/4-}$ with 0.1 M KCl as the supporting electrolyte. Inset is the Randles circuit. (B) CVs of HRP/MUA-MCH/Au (a), Con A/HRP/MUA-MCH/Au (b), HRP/Con A/HRP/MUA-MCH/Au (c), Cyt *c*-HRP/MUA-MCH/Au ($n_{Cyt\ c}/n_{HRP}$=4:1; $n_{Cyt\ c+HRP}$=2.0 nmol) (d), Cyt *c*/Con A/HRP/MUA-MCH/Au ($n_{Cyt\ c}$=2.0 nmol) (e) and Cyt *c*-HRP/Con A/HRP/MUA-MCH/Au ($n_{Cyt\ c}/n_{HRP}$=4:1; $n_{Cyt\ c+HRP}$=2.0 nmol) (f) in N_2-saturated supporting electrolyte solution (pH 9.6). The scan rate: 0.1 V s^{-1}. (C) The plot of peak current versus different molar ratio of $n_{Cyt\ c}/n_{HRP}$ to the Cyt *c*-HRP/Con A /HRP/MUA-MCH/Au ($n_{Cyt\ c+HRP}$=2.0 nmol) modified electrode in N_2-saturated supporting electrolyte solution (pH 9.6). (D) The plot of peak current versus different total number of moles ($n_{Cyt\ c+\ HRP}$) to the Cyt c-HRP/Con A/HRP/MUA-MCH/Au ($n_{Cyt\ c}/n_{HRP}$ = 4:1) modified electrode in N_2-saturated supporting electrolyte solution (pH 9.6). The scan rate: 0.1 V s^{-1}.

The electron transfer process of the resulted electrode was also investigated by CVs. Fig. 4A shows the CVs of the Cyt *c*-HRP/Con A/HRP/MUA-MCH/Au electrode ($n_{Cyt\ c}/n_{HRP}$ = 4:1; $n_{Cyt\ c+HRP}$ = 2.0 nmol) at various scan rates. The cathodic and anodic peak potentials exhibited a small shift caused by the increase in the scan rate (v). At the same time, the peak current (I_p) increased along with the increasing scan rate (0.1 V s^{-1} to 1.0 V s^{-1}) (Fig. 4B). The result indicated that the electrode reaction

involves a surface-controlled quasi-reversible electrochemical process. The electron-transfer coefficient (α_s) and electron-transfer rate constant (k_s) could be determined based on the Laviron theory (Laviron 1979):

$$E_{pc} = E^{o'} + \frac{RT}{\alpha_s nF} - \frac{RT}{\alpha_s nF} \ln v \qquad (1)$$

$$E_{pa} = E^{o'} + \frac{RT}{(1-\alpha_s)nF} + \frac{RT}{(1-\alpha_s)nF} \ln v \qquad (2)$$

Where n is the electron transfer number, R is the gas constant (R = 8.314 J mol^{-1} K^{-1}), T is the temperature in Kelvin (T = 298 K) and F is the Faraday constant (F = 96493 C mol^{-1}). Fig. 4C showed the plots of peak potential (E_{pc}, E_{pa}) versus the natural logarithm of the scan rate (ln υ). When the scan rate varied from 0.75 to 1.0 V s^{-1}, the plots of E_p versus ln υ yielded two straight lines (Fig. 4D) with slopes $-RT/\alpha nF$ and $RT/(1-\alpha)nF$ for the corresponding cathodic and anodic peaks. The αn was calculated to be 1.972 according to the above mentioned slopes. According to the previous literature [34], assume $0.3 < \alpha < 0.7$, it could be concluded that n = 4, and α = 0.49. Therein, the redox reaction of Cyt *c*-HRP in the tri-protein bio-interphase might belong to four electron-transfer process. It is obviously different from the single electron-transfer process of Cyt *c* or HRP [35,36], indicating a synergistic interaction between Cyt *c* and HRP occurred. Assumed single electron transfer in each heme group of Cyt *c* or HRP, we could presume that only four Cyt *c* or HRP molecules took part in the redox reaction. Considered the optimal ratio of Cyt *c* and HRP is 4:1, it is possible to assume that three Cyt *c* and one HRP involved in the redox reaction. Another Cyt *c* molecule might only play an important role in electron shuttling and synergistic interaction between Cyt *c* and HRP. When the $n\Delta Ep$>200 mV, the electron transfer rate k_s could be estimated with the Laviron's equation [37]:

$$k_s = \alpha nFv / RT \qquad (3)$$

At the scan rate of 0.1 V s^{-1}, the mean value of $k_{s,\,(Cyt\ c\text{-}HRP)}$ is calculated to be 7.67±0.22 s^{-1}. The $k_{s,\,(Cyt\ c\text{-}HRP)}$ is much higher than that of other electrodes constructed here (3.82±0.27 s^{-1} for Cyt *c*/Con A/HRP/MUA-MCH/Au electrode, and 2.96±0.18 s^{-1} for Cyt *c*-HRP//MUA-MCH/Au electrode) and our previous results (2.63 s^{-1} for Cyt *c*-HRP//GO-CHIT/Cyt c/MUA-MCH/Au electrode [18] and 7.73±0.22 s^{-1} for Cyt *c*-HRP//DNA/Cyt c/MUA-MCH/Au electrode [24]. The fast electron transfer of Cyt *c*-HRP/Con A/HRP/MUA-MCH/Au electrode might be attributed to the following factors. Firstly, the synergistic interaction between HRP and Cyt *c* might result in an optical protein conformation and porous structure to facilitate electron transfer. Secondly, the electron produced from one protein could transfer to electrode surface by the other protein. Last, the strong biospecific interactions between HRP and Con A might result in a stable structure helping the electron transfer.

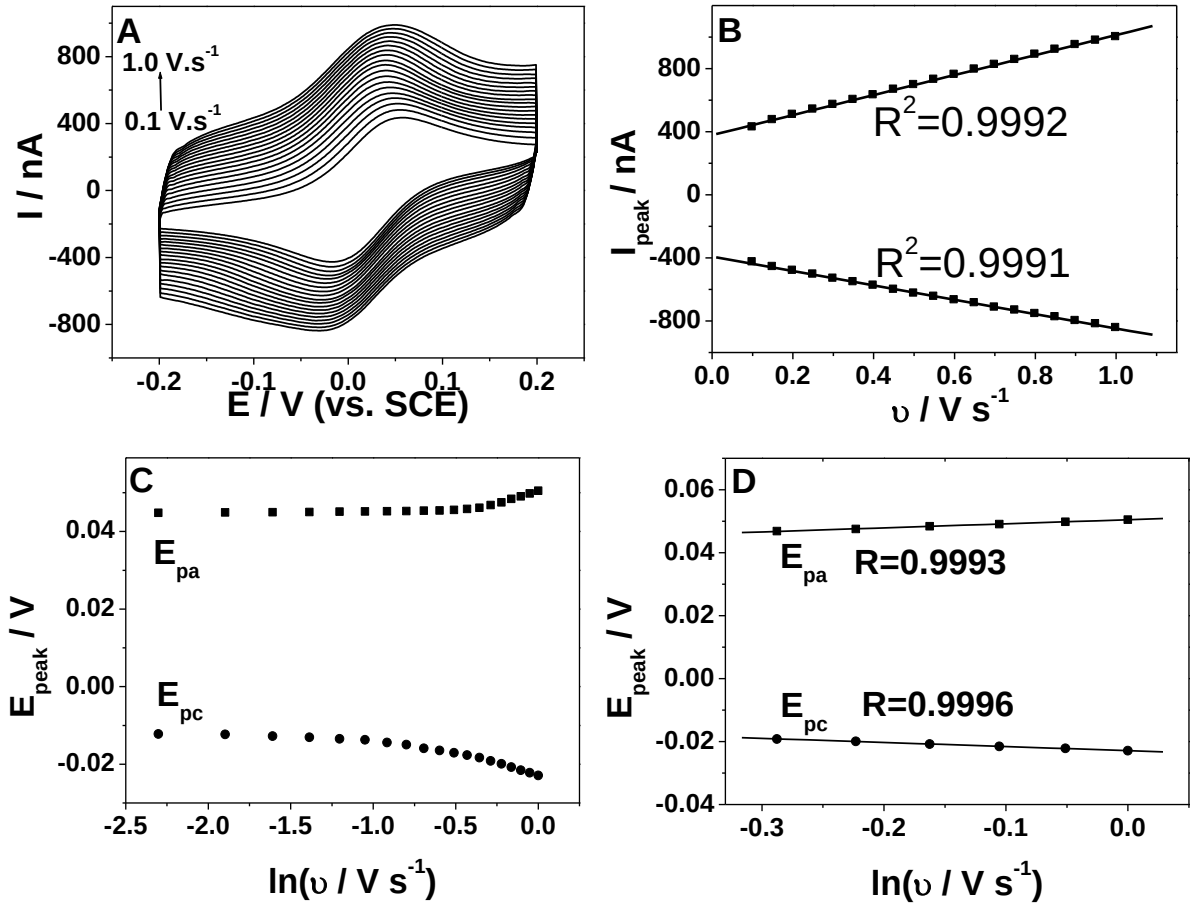

Figure 4.(A) CVs of the Cyt *c*-HRP/Con A/HRP/MUA-MCH/Au ($n_{Cyt\ c}/n_{HRP}$=4:1; $n_{Cyt\ c+HRP}$=2.0 nmol) at different scan rates varied from 0.1 to 1.0 V s^{-1} with a step of 0.05 V s^{-1} in N_2-saturated supporting electrolyte solution (pH 9.6). (B) Plot of I_{peak} versus scan rate (υ). (C) Plots of the peak potential (E_{pa}, E_{pc}) versus the natural logarithm of scan rate (ln υ) and (D) Plot of E_{pa} and E_{pc} versus the natural logarithm of scan rate (ln υ) (υ=0.7, 0.75, 0.8, 0.85, 0.9, 0.95 and 1.0 V s^{-1}).

3.3 Electrocatalytic properties of the tri-protein modified electrodes

The electrocatalytic behaviors of the Cyt *c*-HRP/Con A/HRP/MUA-MCH/Au ($n_{Cyt\ c}/n_{HRP}$ = 4:1; $n_{Cyt\ c+HRP}$ = 2.0 nmol) electrode was investigated towards the reduction of O_2 and H_2O_2. Firstly, the good electrocatalytic activity of the tri-protein electrode towards the reduction of O_2 was discussed (Fig. 5A). At scan rate of 0.005 V s^{-1}, only a small cathodic current was observed in the N_2-saturated supporting electrolyte solution (curve a, Fig. 5A). The cathodic current increased in the presence of air (curve b, Fig. 5A) and further enhanced in the presence of O_2 (curve c, Fig. 5A). The experimental results show the dependence of the cathodic current on the O_2 quantity in the solution at low scan rate, suggesting the tri-protein bio-interphase can be used for the electrocatalytic reduction of O_2.

Fig. 5B shows the bioelectrocatalytic response of tri-protein electrode towards H_2O_2. It can be observed that with the increasing concentration of H_2O_2 (from 0 to 5 mM), the cathodic peak currents

increased dramatically companying by the decrease of the anodic peak, showing a typical electrocatalytic reduction process.

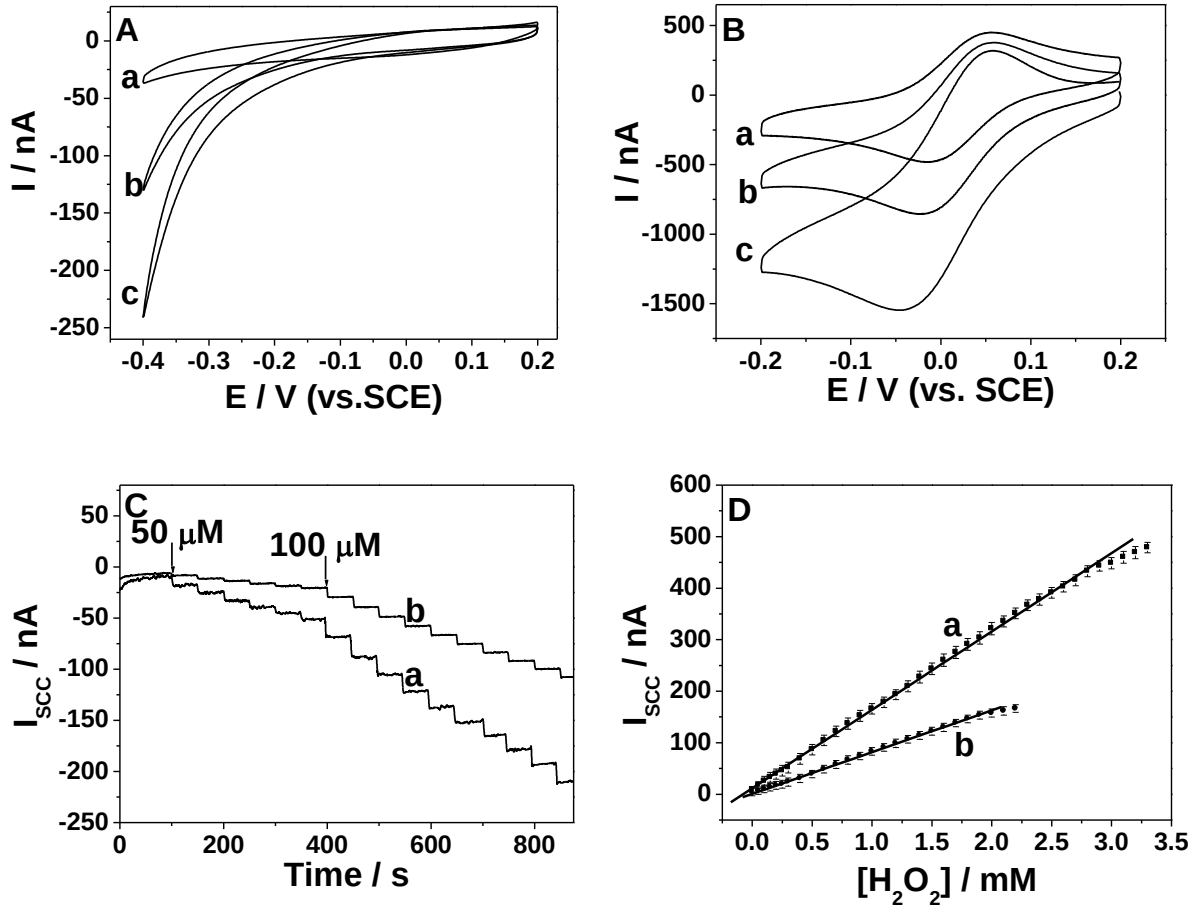

Figure 5.(A) CVs of the Cyt *c*-HRP/Con A/HRP/MUA-MCH/Au electrode ($n_{Cyt\ c}/n_{HRP}$=4:1; $n_{Cyt\ c+HRP}$=2.0 nmol) in N_2-saturated (a), air-saturated (b) and O_2-saturated (c) supporting electrolyte solution (pH 9.6) at the scan rate of 0.005 V s^{-1}. (B) CVs of the Cyt *c*-HRP/Con A/HRP/MUA-MCH/Au ($n_{Cyt\ c}/n_{HRP}$=4:1; $n_{Cyt\ c+HRP}$=2.0 nmol) in N_2-saturated supporting electrolyte solution (pH 9.6) with 0 (a), 2 (b) and 5mM (c) H_2O_2. Scan rate: 0.1 V s^{-1}. (C) Typical steady-state current of the Cyt *c*-HRP/Con A/HRP/MUA-MCH/Au ($n_{Cyt\ c}/n_{HRP}$=4:1; $n_{Cyt\ c+HRP}$=2.0 nmol) electrode (a), Cyt *c* /Con A/HRP/MUA-MCH/Au ($n_{Cyt\ c}$ =2.0 nmol) electrode (b) to successive injection of H_2O_2 into 10 mL of stirring supporting electrolyte solution (pH 9.6), respectively. (D) Calibration curve between current and the concentration of H_2O_2. Applied potential: -0.05 V.

The bioelectrocatalysis of the tri-protein electrode was further characterized by amperometry. Fig. 5C shows the comparison between current-time curves of the Cyt *c*-HRP/Con A/HRP/MUA-MCH/Au (n_{Cytc}/n_{HRP} = 4:1; $n_{Cytc+HRP}$ = 2.0 nmol) (curve a) electrode and the Cyt *c*/Con A/HRP/MUA-MCH/Au ($n_{Cyt\ c}$= 2.0 nmol) (curve b) electrode towards the reduction of H_2O_2. The amperometric responses of the biosensors were studied by the successive additions of the H_2O_2 in the supporting electrolyte solution (pH 9.6) at an applied potential of -0.05 V (vs. SCE) under stirring. With the

successive addition of H_2O_2, the stepped increases of the amperometric reduction currents were observed. The reduction current rose sharply to reach a maximum steady-state value and achieved 97% of the steady-state current (I_{ssc}) within 2 s for both electrodes. Fig. 5D shows the calibration curve of the biosensor. The linear range of the H_2O_2 detection was from 0.02 to 3.0 mM (R = 0.9996; n = 31) for the Cyt *c*-HRP/Con A/HRP/MUA-MCH/Au ($n_{Cyt\ c}/n_{HRP}$ = 4:1; $n_{Cyt\ c}+n_{HRP}$ = 2.0 nmol) electrode (curve a). The detection limit was estimated to be 7.83 μM based on the criterion of a signal-to-noise ratio of 3, and the sensitivity was 0.152 μA/mM (Fig. 5D, curve a). The results were obviously superior to previous results [18,24] (Table 1).

Table 1. Comparison of the performance of various H_2O_2 sensors constructed from Cyt *c* and HRP.

	Detection limit (μM)	Linear range (mM)	[a]k_s (s^{-1})	Reproducibility (RSD,%)		References
Cyt *c*-HRP/Con A/HRP/MUA-MCH/Au	7.83	0.02-3.0	7.67	[b]2.97	[c]3.64	This work
Cyt *c*-HRP/CHIT-GO/Cyt *c*/MUA-MCH/Au	6.68	0.02-0.33	2.63	4.21	4.62	[18]
Cyt *c*-HRP/DNA/Cyt *c*/MUA-MCH/Au	27.3	0.05-0.90	7.73±0.38	4.18	5.50	[24]
Cyt *c*/Nanoporous Au	6.3	0.01-12	3.9	—	7.2	[38]
Cyt *c*-PAN-ALA/GCE	8.2	0.025-0.3	[d]1.9	3.7	4.2	[36]
HRP-SAM-AuNAE$_{5h}$	0.42	0.74-15	2.22	—	4.6	[35]
HRP/laponite/CHIT/GCE	5	0.029-1.4	1.82	—	—	[39]

[a] k_s was estimated at 0.1 V/s;
[b] The same electrode;
[c] Electrode-to- electrode;
[d]The average k_s.

For comparison, the determination of H_2O_2 using Cyt *c* /Con A/HRP/MUA-MCH/Au ($n_{Cyt\ c}$ = 2.0 nmol) is also listed (curve b). At Cyt *c*/Con A/HRP/MUA-MCH/Au electrode, relatively low amperometric response was observed when H_2O_2 was added to the stirring supporting electrolyte solution. The linear range of the H_2O_2 detection was found to be 0.04 to 2.1 mM (R = 0.9997; n = 21) with sensitivity of 0.082 μA/mM. A detection limit of 14.2 μM can be estimated based on the criterion of a signal-to-noise ratio of 3. The comparison between Cyt *c* /Con A/HRP/MUA-MCH/Au and Cyt *c*-HRP/Con A/HRP/MUA-MCH/Au electrode declared that the tri-protein electrode possessed a better catalytic activity and sensitivity towards the reduction of H_2O_2. The good catalytic activity and sensitivity might result from the synergistic interactions between the two proteins.

3.4 Selectivity, stability, repeatability and reproducibility of the bi-protein modified electrode

The selectivity of the sensor was examined by sequential additions of 0.1 mM H_2O_2, 2.0 mM ascorbic acid (AA) and 2.0 mM uric acid (UA) into the stirring supporting electrolyte solution (pH 9.6). The results indicated that AA and UA had no obvious interference in the detection of H_2O_2 at the studied concentration. The stability of the Cyt *c*-HRP/Con A/HRP/MUA-MCH/Au biosensor was evaluated by monitoring the response currents in the presence of 2 mM H_2O_2 over 7 days period. The

modified electrode was stored in PBS at 4°C in a refrigerator and measurements were repeated every day. The biosensor retained about 97.85% of the original response, and the peak potentials remained constant, respectively. The repeatability and reproducibility of the current signal for the same electrode and electrode-to-electrode was 2.97% and 3.64% (RSD, n = 5), respectively. The stability, repeatability and reproducibility were superior to previous results [18,24] (Table 1).

4. CONCLUSIONS

Cyt *c*-HRP/Con A/HRP films were successfully assembled onto the MUA-MCH modified Au electrode through biospecific complexation between Con A and glycoprotein HRP, combined with electrostatic interactions between HRP and Cyt *c*. The superior design of introducing mixed proteins to the modified electrode greatly promoted the electron transfer. The tri-protein electrode exhibited fast electron transfer and good electrocatalytic activity towards the reduction of H_2O_2 and O_2. Moreover, the established biosensor showed fast amperometric response, low detection limit and wide linear range towards the reduction of H_2O_2. The results were obviously superior to our previous bi-protein results. This study also provided new insights for the electron transfer of multi-proteins in a bio-interphase and the development of biosensors.

ACKNOWLEDGEMENT
This work was financially supported by National Natural Science Foundation of China (20905032, 21065005, 21165010), Young Scientist Foundation of Jiangxi Province (20112BCB23006), Foundation of Jiangxi Educational Committee (GJJ10389), the State Key Laboratory of Electroanalytical Chemistry (2008003), Scientific Research Foundation for the Returned Overseas Chinese Scholars, the Open Project Program of Key Laboratory of Functional Small organic molecule, Ministry of Education, Jiangxi Normal University (No. KLFS-KF-201214; KLFS-KF-201218), State Education Ministry and Innovation Foundation for graduate student of Jiangxi Province (YC2011-S037).

References

1. Y.M. Yan, I. Baravik, O. Yehezkeli, I. Willner, *J. Phys. Chem. C*, 112(2008) 17883.
2. K.M. Manesh, P. Santhosh, S. Uthayakumar, A.I. Gopalan, K.P. Leea, *Biosens. Bioelectron.*, 25(2010) 1579.
3. Y.H. Song, L.L. Wan, K. Cui, L. Liu, M. Zhang, J. Liao, L. Wang, Z. Li, *J. Electroanal. Chem.*, 656(2011) 206.
4. Y.M. Yan, R. Tel-Vered, O. Yehezkeli, Z. Cheglakov, I. Willner, *Adv. Mater.*, 20(2008) 2365.
5. O. Yehezkeli, R. Tel-Vered, S. Raichlin, I. Willner, *ACS Nano*, 5(2010) 2385.
6. Y. Xiao, F. Patolsky, E. Katz, J. F. Hainfeld, I. Willner, *Science*, 299(2003) 1877.
7. R. Freeman, B. Willner, I. Willner, *J. Phys. Chem. Lett.*, 2(2011) 2667.
8. M. Zheng, Y. Cui, X.Y. Li, S.Q. Liu, Z.Y. Tang, *J. Electroanal. Chem.*, 656(2010) 167.
9. X.Y. Li, Y.L. Zhou, Z.Z. Zheng, X.L. Yue, Z.F. Dai, S.Q. Liu, Z.Y. Tang, *Langmuir*, 25(2009) 6580.
10. L.H. Jin, L. Shang, S.J. Guo, Y.X. Fang, D. Wen, L. Wang, J.Y. Yin, S.J. Dong, *Biosens.*

Bioelectron., 26(2011) 1965.
11. S. Cosnier, C. Mousty, X. Cui, X. Yang, S. Dong, *Anal. Chem.*, 78(2006) 4985.
12. L.D. Zhu, R.L. Yang, J.L. Zhai, C.Y. Tian, *Biosens. Bioelectron.*, 23(2007) 528.
13. R. Dronov, D.G. Kurth, H. Möhwald, F.W. Scheller, F. Lisdat, *Electrochim. Acta*, 53(2007) 1107.
14. R. Dronov, D.G. Kurth, H. Möhwald, F.W. Scheller, F. Lisdat, *Angew. Chem. Int. Ed.*, 47(2008) 3000.
15. R. Dronov, D.G. Kurth, H. Möhwald, R. Spricigo, S. Leimkühler, U. Wollenberger, K.V. Rajagopalan, F.W. Scheller, F. Lisdat, *J. Am. Chem. Soc.*, 130(2008) 1122.
16. T.H. Balkenhohl, S. Adelt, R. Dronov, F. Lisdat, *Electrochem. Commun.*, 10(2008) 914.
17. F. Wegerich, P. Turano, M. Allegrozzi, H. Möhwald, F. Lisdat, *Langmuir*, 27(2011) 4202.
18. L.L. Wan, Y.H. Song, H.Z. Zhu, Y. Wang, L. Wang, *Int. J. Electrochem. Sci.*, 6(2011) 4700.
19. C. Yang, C. Xu, X. Wang, *Langmuir*, 28(2012) 4580.
20. J. Fu, M. Liu, Y. Liu, N.W. Woodbury, H. Yan, *J. Am. Chem. Soc.*, 134(2012) 5516.
21. S.A. Mozaffari, T. Chang, S.M. Park, *J. Phys. Chem. C*, 113(2009) 12434.
22. K. Nakano, T. Yoshitake, Y. Yamashita, E.F. Bowden, *Langmuir*, 23(2007) 6270.
23. M.K. Beissenhirtz, F.W. Scheller, W.F.M. Stöcklein, D.G. Kurth, H. Möhwald, F. Lisdat, *Angew. Chem. Int. Ed.*, 43(2004) 4357.
24. Y.H. Song, L.L. Wan, Y. Wang, S.C. Zhao, H.Q. Hou, L. Wang, *Bioelectrochemistry*, 85(2012) 29.
25. J.W. Becker, G.N. Reeke Jr, B.A. Cunningham, G.M. Edelman, *Nature*, 259(1976) 406.
26. H. Yao, N. Hu, *J. Phys. Chem. B*, 114(2010) 3380.
27. H. Yao, N. Hu, *J. Phys. Chem. B*, 114(2010) 9926,.
28. H. Yao, N. Hu, *J. Phys. Chem. B*, 115(2011) 6691.
29. G. Liu, Y. Lin, *Anal. Chem.*, 78(2006) 835.
30. Y. Kobayashi, T. Hoshi, J. Anzai, *Chem. Pharm. Bull.*, 49(2001) 755.
31. Y. Song, L. Wang, C. Ren, G. Zhu, Z. Li, *Sensor. Actuator. B–Chem.*, 114(2006) 1001.
32. H.O. Finklea, D.A. Snider, J. Fedyk, E. Sabatani, Y. Gafni, I. Rubinstein, *Langmuir*, 9(1993) 3660.
33. R. Swanson, B.L. Trus, N. Mandel, G. Mandel, O.B. Kallai, R.E. Dickerson, *J. Biol. Chem.*, 252(1977) 759.
34. H.Y. Ma, N.F. Hu, J.F. Rusling, *Langmuir*, 16(2000) 4969.
35. J. Xu, F. Shang, J.H.T. Luong, K.M. Razeeb, J.D. Glennnon, *Biosens. Bioelectron.*, 25 (2010) 1313.
36. L. Zhang, Z. Shi, Q. Lang, J. Pan, *Electrochem. Acta*, 55(2009) 641.
37. E. Laviron, *J. Electroanal. Chem.*, 101(1979) 19.
38. A. Zhu, Y. Tian, H. Liu, Y. Luo, *Biomaterials*, 30 (2009) 3183.
39. D. Shan, Q. B. Li, S.N. Ding, J.Q. Xu, S. Cosnier, H.G. Xue, *Biosens. Bioelectron.*, 26(2010) 536.